L1C COMPARISON OF IASI-A AND IASI-B ON METOP SATELLITES: MONITORING OF RADIOMETRIC AND SPECTRAL PERFORMANCES AND POSSIBLE USE FOR CLIMATE STUDIES

C. Camy-Peyret[(1)], J. Bureau[(2)], D. Coppens[(3)], B. Théodore[(3)] and T. August[(3)]

[(1)]IPSL, UPMC et UVSQ, Box 101, 4 Place Jussieu, 75252, Paris cedex 05, France
[(2)]LATMOS, Université Pierre et Marie Curie, 4 Pl. Jussieu, 75252, Paris cedex 05, France
[(3)]EUMETSAT, Eumetsat-Allee 1, 64295 Darmstadt, Germany

Abstract

A method is presented to compare the L1c products (calibrated radiance spectra) of the two IASI (Infrared Atmospheric Sounding Interferometer) instruments on board the two Metop satellites Metop-A and Metop-B. After defining categories of homogenous geophysical/geographical conditions (day/night, ocean/night, clear/overcast), one can produce grand average spectra with the corresponding statistical diagnostics on the L1c spectral grid (8461 channels between 645 and 2760 cm^{-1} with a spacing of 0.250 cm^{-1}).
The corresponding spectra are generated monthly for the 30 scan positions (SP) of the scene acquisition mirror and for the 4 pixels (PN or IFOV) of the two IR sounders. These average spectra (with a much reduced noise as compared to one individual IASI spectrum) and the corresponding uncertainty on a channel-by-channel basis (with a Gaussian character check) can then be used to compare the two instruments on the short time scale (month or shorter periods). A pixel-by-pixel comparison of IASI-A and IASI-B is not possible because the two instruments can never "see" the same footprint at the same time, since they are flying 50 min apart on the same orbit. But due to this small time difference, the set of sampled IFOVs used for generating the averages (over given homogeneous categories) should obey the approximation <IASI-A - IASI-B> ≅ <IASI-A> - <IASI-B>. The left term of the equation would be the hypothetical pixel-by-pixel spectral radiance difference of the two sounders if they were sampling the same footprint at the same time. The right hand side term is the difference calculated from the mean of the individual sounders calculated for the various categories over a given time period. A status on the efforts to implement this tool in the EPS monitoring environment and the potential for instrument as well as climate monitoring is presented.

INTRODUCTION

The inter-comparison of IASI-A and IASI-B has two objectives:

- to monitor the quality of L1c IASI products disseminated by EUMETSAT (Coppens *et al.*, 2013);
- to demonstrate that IASI can be used in the GSICS framework: IASI-A has indeed proved to be an excellent reference (Chinaud *et al.*, 2013) and the commissioning of IASI-B (Jacquette *et al.*, 2013) has shown that both instruments are of similar quality, IASI-B now being the primary instrument in the morning orbit since 24 April 2013.

Such an inter-comparison can be performed using two approaches:

- an indirect comparison using a third reference, namely the double-differences technique. Several studies have been conducted using SST observations from a third satellite, often geostationary, as reference (see for instance, Wang *et al.*, 2010). Other inter-comparisons have been using a calculated spectrum as third element of the differences (see for instance, Elliot *et al.*, 2009; Jouglet *et al.*, 2013; Théodore *et al.*, 2013). The near real time monitoring of L1c IASI radiances at Eumetsat is also based on this method (Coppens *et al.*, 2013);
- a direct comparison of the average spectra, the averaging process being performed over consistent geophysical and temporal conditions.

The present paper is a preliminary work in this direction. The basic assumption is that the IFOVs sampled by IASI-A and IASI-B belong to the same underlying statistical distributions (within relevant categories). Combined to the large number of spectra averaged within each category, one can then assume that the difference of average spectra is equivalent to the average of the IFOV by IFOV difference of both sounders. In all instances it is not possible to perform this operation exactly because of the 50 minutes lag of Metop-A and Metop-B on the same orbit. The assumption is then (on a category by category basis) that:

$$\langle \text{IASI-A - IASI-B} \rangle \cong \langle \text{IASI-A} \rangle - \langle \text{IASI-B} \rangle$$

This is the justification of the separate calculation of average spectra within appropriate spatial categories (over which geophysical conditions are assumed to be identical and stationary). Examination of the individual results for <IASI-A> and <IASI-B> is of interest by itself. An IFOV by IFOV comparison (with 50 min difference anyway) would be much more cumbersome to compute. Starting from average spectra one can search for very small radiometric and spectral differences between the two instruments. Or one can also check for inter-annual differences by comparing average spectra (of a given geophysical category) for the same month but successive years, thus contributing to climate change studies.

CATEGORIES FOR THE COMPARISON

The native EPS format files are used to generate average L1c spectra within given categories (or boxes) for further statistical analysis. The method works "in stream" i.e. the computation of the statistical average and of the higher moments does not require to store all individual spectra in memory but needs just a single pass over each file since the statistical parameters of the underlying distribution are updated for each new spectrum assigned to the appropriate category. A tool for testing the Gaussian character of the average spectra (on a channel by channel and category by category basis) allows us to draw meaningful conclusions based on the large number of IFOVs in the averaging process.
Categories (or boxes) are used to divide the huge ensemble of available spectra into homogeneous subsets from which a random sampling (or draw) for generating averages can be considered as statistically representative. A category is defined according to the following criterions:

- latitude (subscript `il`), `il`=[1,2,3,4,5] → [SH-polar, SH-mid, tropical, NH-mid, NH-polar]
- scan position or nadir angle (SP, subscript `ia`), `ia`=[1;30] → all scan mirror positions
- pixel number (PN, subscript `ip`), `ip`=[1,2,3,4] → 4 pixels within a given FOR
- ground or surface type (subscript `ig`), `ig`=[1,2] → land or water
- solar zenith angle (subscript `is`), `is`=[1,2] → day or night
- nebulosity or cloud coverage (subscript `ic`), `ic`=[1,2] → clear or overcast

For latitude bands, the limits used are -90.0°, -60.0°, -20.0°, 0.0°, 20.0°, 60.0°, 90.0°. For land fraction, the limits are: 1 → land 0.99 ≤ `landfrac` ≤ 1.00; 2 → water 0.00 ≤ `landfrac` ≤ 0.01. For solar zenith angle, the limits are: 1 → day, SZA ≤ 118°; 2 → night, SZA > 118°. For nebulosity, the cloud fraction limits (AVHRR product within IASI L1c) are: 1 → clear 0.00 ≤ `cloudfrac` ≤ 0.02; 2 → overcast 0.98 ≤ `cloudfrac` ≤ 1.00. All IFOVs not falling into these criterions (mixed or intermediate cases) are not retained in the averaging process.

The additional subscript within a given category is the IASI L1c channel number (index `ix`=[1;8461]) with wavenumbers in cm^{-1} σ(`ix`)=645.00+0.25×(`ix`-1). The corresponding average spectral radiance arrays are then of type `rad(il,ia,ip,ig,is,ic,ix)`. Similar arrays are generated for the standard deviation `stdv` (rms around the mean), for the skewness and for the kurtosis (`skew` or `kurt` i.e. 3rd and 4th order moments) as well as for the extreme values (`rmin`, `rmax`). The number of subscripts and the range of possible values for the indices is an indication of the scale (memory and storage resources) of the exercise. The array size is then 5×30×4×2×2×2×8461= 40612800. That means for 6 arrays (`rad,stdv,skew,kurt,rmin,rmax`) of double precision values a memory of 40612800×6×8 = 1949414400 ~ 1.95 GB. One additional integer array is such that `ig(ix)`=0 if the

channel has indeed a Gaussian character as derived from the observed values of `skew(il,ia,ip,ig,is,ic,ix)` and `kurt(il,ia,ip,ig,is,ic,ix)`. The overall spectra of IASI-A and IASI-B for the category SP=18, tropical, water, night, clear are shown in Figure 1.

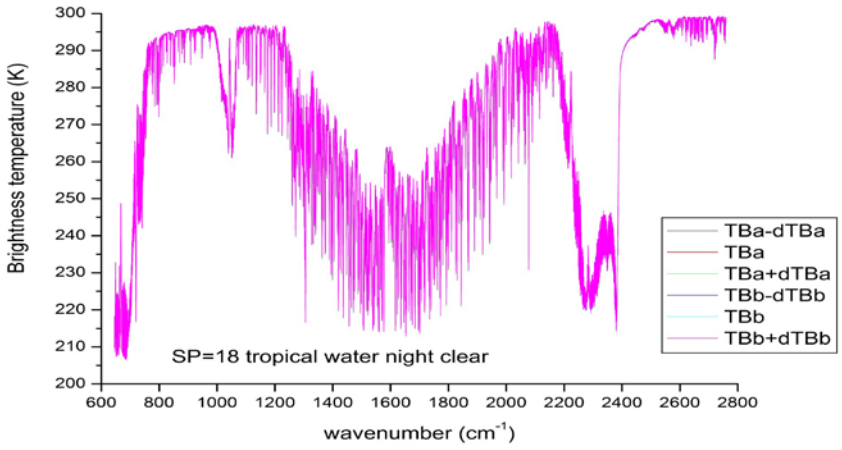

Figure 1: **Overall spectra of a= IASI-A and b=IASI-B for the category SP=18, tropical, water, night, clear (the average and the average ± the uncertainty are plotted for both sounders). The differences are barely visible. Note that TB=Brightness Temperature; dTBa and dTBb are the statistical uncertainties (1σ) on the mean spectra TBa and TBb.**

An extract covering the CO_2 laser band and a further zoom around 937 cm^{-1} are shown in Figure 2.

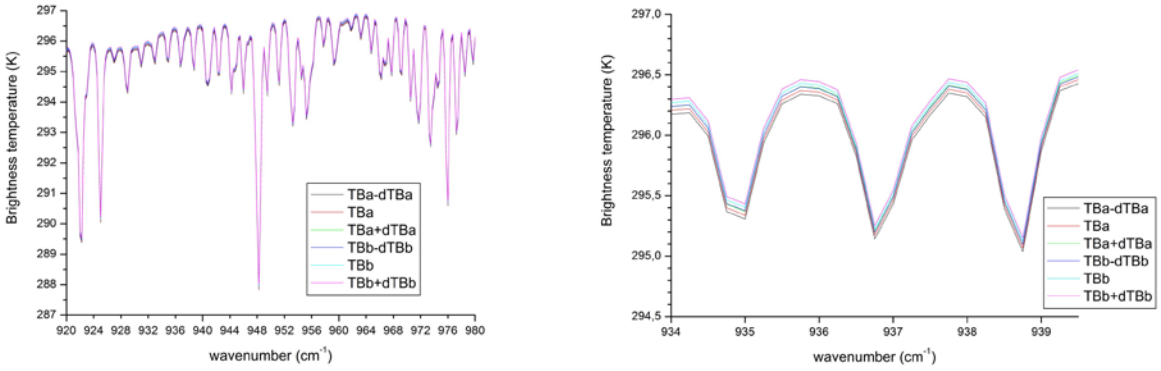

Figure 2: **Same as in Figure 1, except for a zoom over the CO_2 laser band (left) and a further zoom (right) around 937 cm^{-1}. A small bias of about 0.1 K is observable (IASI-B being slightly warmer). Data for Feb/March during the commissioning phase when the IASI-B configuration was not yet optimized.**

RELATIVE SPECTRAL CALIBRATION FACTORS

Before comparing the radiometry, it is important to check that the (average in our case) spectra of the two sounders are indeed co-aligned on the nominal wavenumber grid σ(ix) with ix=[1;8461] of L1c. A method (called ANA for "analytical") has been developed in previous studies (spectral calibration of MIPAS-Envisat and IASI-balloon Fourier transform spectra) for determining the absolute (with respect to a calculated spectrum) or the relative (between two similar measured spectra) spectral calibration factors $\varepsilon=\delta\sigma/\sigma$. This method was re-furbished (adapted to IASI) for comparing the relative spectral calibration of average IASI-A and IASI-B spectra. We present briefly below a demonstration of the method as applied to an average spectrum (called a) of IASI-A (same category as for Figure 1) which has been spectrally scaled by $\varepsilon=\pm 5\times10^{-6}$ to generate modified spectra (called c) such that $c(\sigma) \sim a([1+\varepsilon]\sigma)$. The spectra are plotted in Figure 3 (vicinity of the Q branch of the CO_2 ν_2 band) and the brightness temperature differences are plotted in Figure 4. TBa is the initial unscaled (spectrally) brightness temperature spectrum is identical to TBc(0).

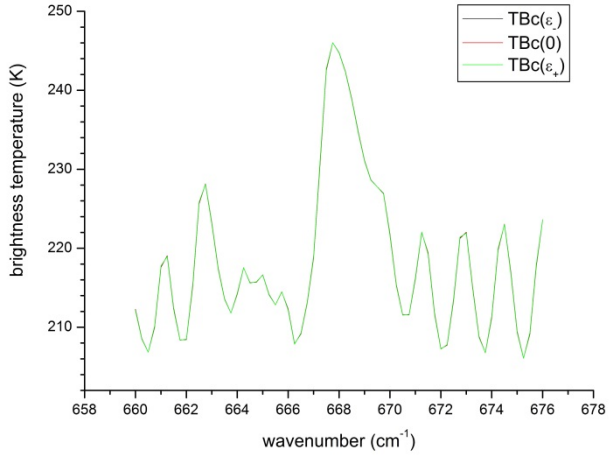

Figure 3: **IASI-A spectrum (TBc(0) no scaling factor) and spectrally scaled spectra (TBc(ε_-) with with ε=-5×10^{-6} and TBc(ε_+) with ε=+5×10^{-6}). The differences are not detectable here.**

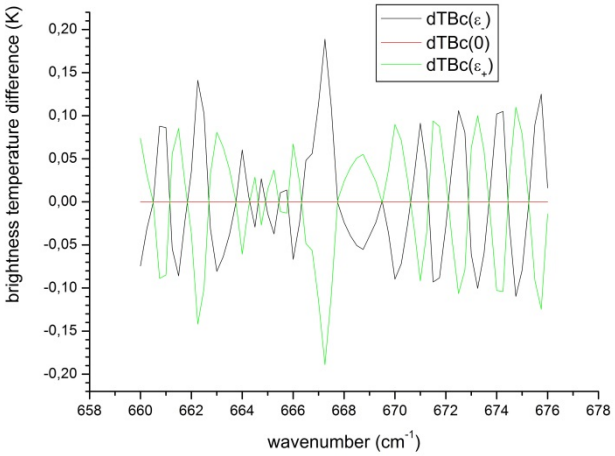

Figure 4: **Same as in Figure 3, except that differences of TBc(ε_-) and TBc(ε_+) with respect to TBc(0) are plotted. The maximum brightness temperature differences are of the order of ±0.2 K. This is demonstrating the sensitivity (hence the need for averaging) necessary for a good determination of the scaling factors ε.**

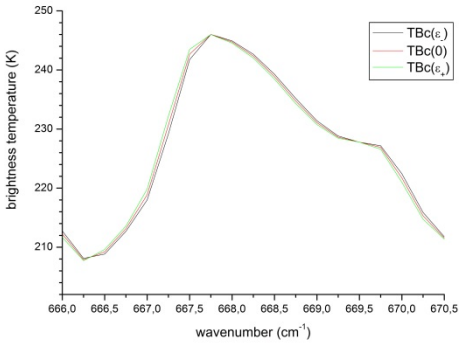

Figure 5: **Effect of the application of large scaling factors (TBc(ε_-) with ε=+5×10^{-5} and TBc(ε_+) with ε=-5×10^{-5}, which are unrealistic with respect to IASI specifications) to demonstrate the induced spectral shift, small but visible herewith respect to the initial spectrum TBc(0). The wavenumber grid (nominal one for L1c spectra) is the same for the 3 spectra.**

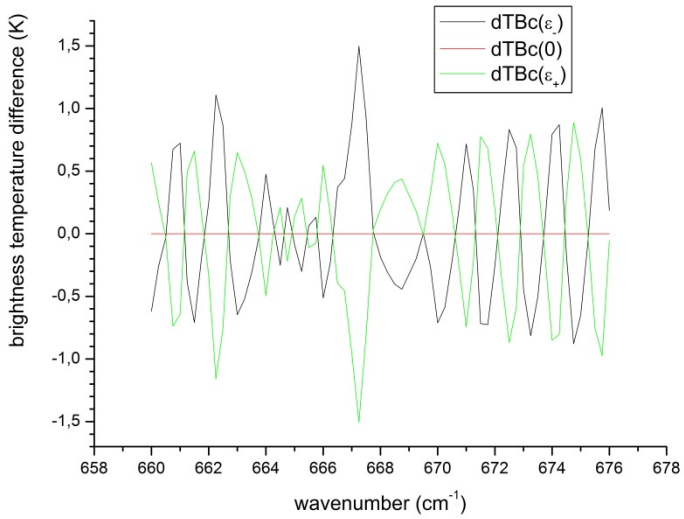

Figure 6: **Same as in Figure 6, but for brightness temperature differences. The differences of TBc(ε-) or TBc(ε+) with respect to TBc(0) (no scaling factor) are here of the order ±1.5 K.**

The algorithm for the determination of the spectral scaling factors has been tested in the above conditions (retrieving the applied ε within numerical noise) and then applied to pairs of average IASI-A and IASI-B spectra for the same months since April 2013. One has to realise that the derived spectral scaling factors are relative ones (IASI-A with respect to IASI-B) and not absolute ones with respect to an exact/accurate forward model simulation. Our initial goal was to compare the two sounders on a monthly basis and will be later to compare the average spectra for the same month (for a given category) on a year to year basis. An example of the distributions of longitudes and integrated equivalent brightness temperature (T_{rad} i.e. the temperature of the blackbody having the same integrated radiance over the full IASI range of 645-2760 cm^{-1}) of the spectra (4945 for IASI-A and 5274 for IASI-B) retained for computing the averages are shown in Figure 7 for PN1 and SP=18 and the month of Aug. 2013. Only categories with correlations in longitude and T_{rad} greater than 95% were considered for deriving the relative spectral calibration factors.

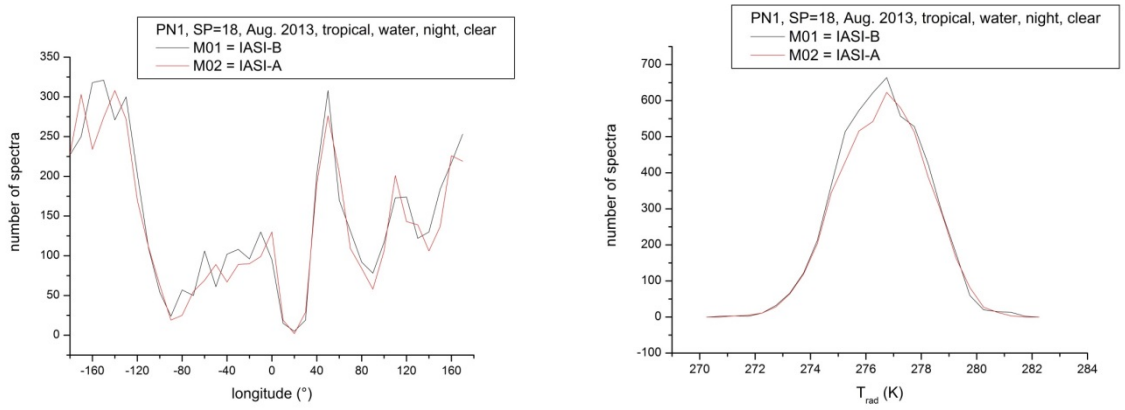

Figure 7: Comparison of the distribution of longitudes (left) and integrated equivalent brightness temperatures (right) of IASI spectra selected for computing the averages for Aug. 2013 and for the category tropical, water, night, clear.

In the initial processing of monthly data, a suspicious transition of the retrieved ε was observed for May, but it was realized, after analysis, that configuration changes did occur for both instruments at mid-month. This is shown in Figure 8 for the 4 IFOVs (or pixels) of IASI. In all cases the derived values of ε are well within the nominal IASI spectral calibration requirement of $|\varepsilon=\delta\sigma/\sigma| < 2\ 10^{-6}$. Firstly it is to be noted that there is a good consistency between the ε values derived separately from the 3 bands of IASI (with a possible larger difference in B1). Secondly, once the configuration change is accounted

for, the stability for the different months of the relative spectral scaling factors is quite good demonstrating that IASI-B has very similar performances (and maybe better) as IASI-A.

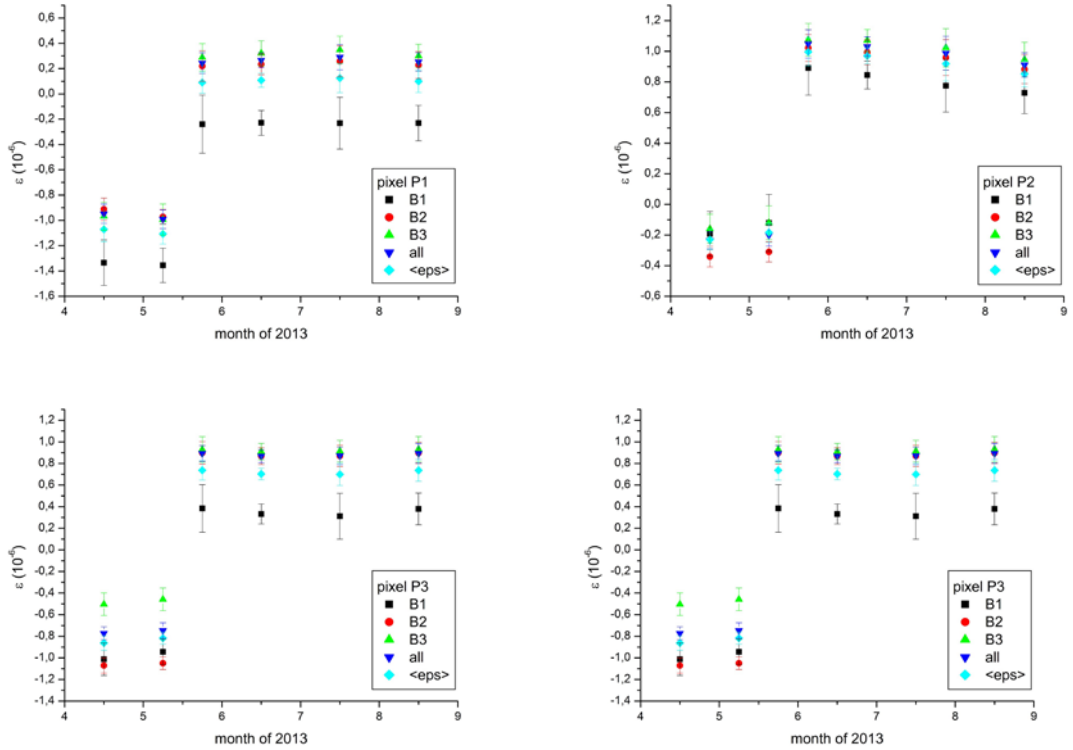

Figure 8: **Evolution of the relative spectral scaling factor (in ppm unit) between IASI-A and IASI-B. The step for May correspond to an on-ground processing update at mid-month. The ε values are changing in the right direction (closer to zero) showing an improvement in the fine tuning of the processing parameters as proposed by the Technical Expertise Centre (TEC).**

RELATIVE RADIOMETRIC DIFFERENCES

We have seen that the impact of the small residual spectral scaling factor between the two sounders is well within the specifications and has a small effect on the radiometry. Thus we have not tried (at this point) to apply the corresponding scaling on the spectra. We have just examined the differences between the average spectra (on a monthly basis again) in combination with the *a priori* uncertainty of the difference (with its spectral dependency) derived from the root sum square of the uncertainty on the mean of each average spectrum. This is shown in Figure 8. The differences are very consistent with the expected error demonstrating the excellent radiometric consistency between the two sounders. The differences are well within the combined radiometric noise of the two instruments (except possibly for some remaining geophysical variability possibly impacting the regions of strong H_2O absorption and for some highly temperature sensitive regions like the band head of the ν_3 band of CO_2 near 2380 cm^{-1}).

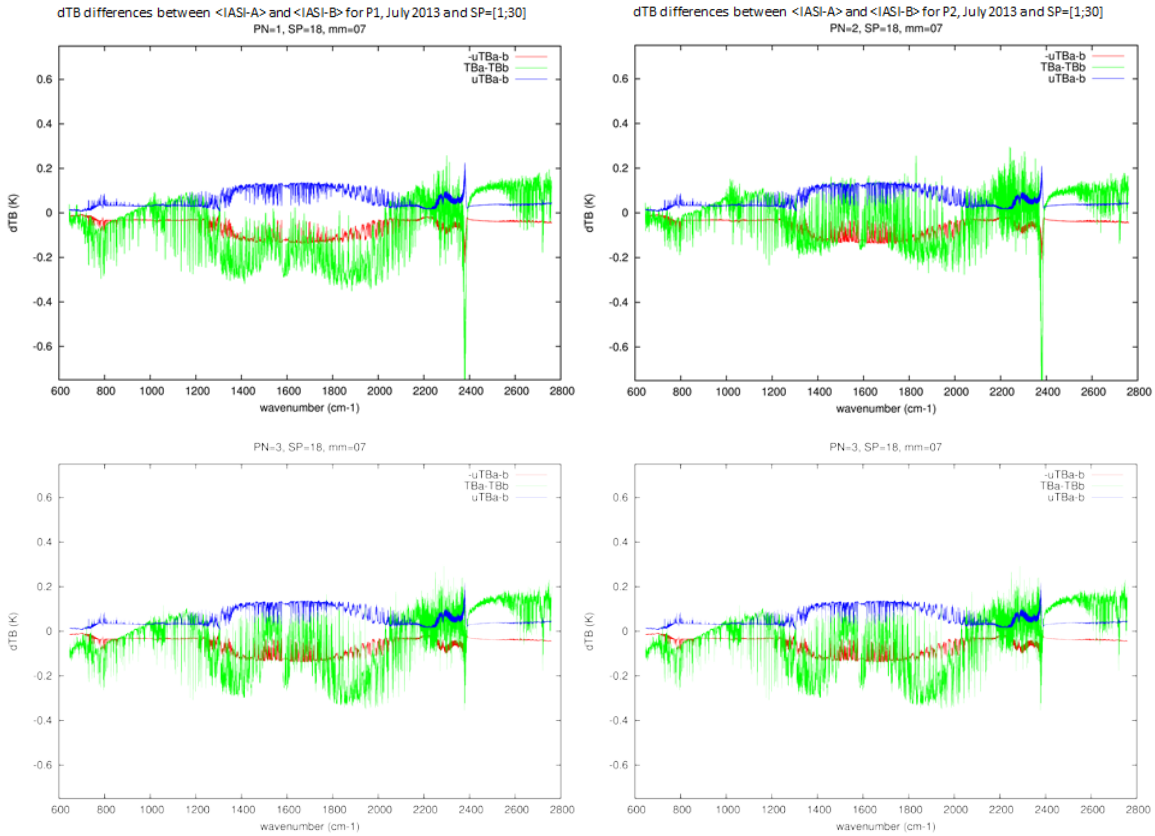

Figure 8: **Brightness temperature differences (between IASI-A and IASI-B) for the 4 IASI pixels and the month of July 2013. The red and blue curves are ± 1σ (one standard deviation) derived from the combined *a priori* uncertainties on the average spectra). The green curve is the observed difference spectrum (no relative spectral scaling factor applied). Note that in general the differences are consistent with the 1σ uncertainty, except for a small region around 2380 cm^{-1} where some geophysical variability related to the temperature profile may remain.**

The overall radiometric differences (bias) between IASI-A and IASI-B have been calculated for the 5 months considered in this analysis (all pixels, all scan positions and the category tropical, water, night, clear). They are all smaller (in absolute value) than 0.07, 0.11 and 0.08 K for the 3 bands of IASI i.e. B1, B2, B3 (respectively), with root mean square (rms) differences (in the same bands) smaller than 0.22, 0.34 and 0.22 K (respectively). Part of these may still be due to some geophysical variability since the IFOVs retained for comparison are not sampling exactly the same underlying statistical distributions at the same time.

CONCLUSION

An excellent consistency (spectrally and radiometrically) between IASI-A and IASI-B has been demonstrated without the use of RTM. A software is in place in test mode at EUMETSAT for running the code every calendar month for IASI-A and IASI-B. Analyses will be pursued to understand possible differences and small evolutions in the spectral scaling factors. The mid-May (abrupt) change is understood and related to configuration changes. Spectral scale corrections could be applied (if needed) once the proper correcting ε(PN,SP) are defined. This could possibly further reduce the radiometric differences between the two sounders. Significant differences in brightness temperature are still around 2380 cm^{-1} and may be related to a remaining variability (beating the IASI noise) due to the strong temperature dependence of the spectral signatures in this latter region. Stricter criterions for selecting the IFOVs of IASI-A and IASI-B retained in each category (test of the IFOV heterogeneity, correlation of the latitude distributions of the 2 sounders within a zonal band,…) will be applied to understand this feature in the differences.

ACKNOWLEDGEMENTS

EUMETSAT is acknowledged for providing support to the first two authors as visiting scientists. CNES, industry and TEC are to be congratulated for designing, manufacturing and maintaining the IASI instruments in extremely good operational conditions. CNES/INSU has been supporting the participation of the first author to this conference.

REFERENCES

Chinaud, J., (2013) IASI quarterly performance report from 2013/03/01 to 2013/05/31. Available at http://smsc.cnes.fr/IASI/Fr/lien1_car_instr.htm

Coppens, D., et al., (2013) Dual IASI-A and IASI-B automatic monitoring for the Level 1 and Level 2. *Poster 10 at this conference*.

Elliott, D. A., *et al*., (2009) Two-year comparison of radiances from the Atmospheric Infrared Sounder (AIRS) and the Infrared Atmospheric Sounding Interferometer (IASI). *Proc. SPIE Int. Soc. Opt. Eng*., **7456**, doi:10.1117/12.826996.

Jacquette, E., *et al.*, (2013) IASI on MetOp-B performance status. *These proceedings.*

Jouglet, D., *et al.*, (2013) Radiometric inter-comparison of IASI: IASIA/IASI-B, IASI/AIRS, IASI/CrIS. *Poster 158 at this conference*.

Théodore, B. and Coppens, D. (2013) Intercomparison of IASI and CrIS spectra. *These proceedings.*

Wang, L. X., *et al*., (2010) Comparison of AIRS and IASI radiance measurements using GOES imagers as transfer radiometers. *J. Appl. Meteorol. Climatol.*. **49**, 478.